AIAA JOURNAL
Vol. 45, No. 7, July 2007

Space Frames with Multiple Stable Configurations

T. Schioler* and S. Pellegrino†
University of Cambridge, Cambridge, CB2 1PZ England, United Kingdom

DOI: 10.2514/1.16825

This paper is concerned with beamlike space frames that include a large number of bistable elements, and exploit the bistability of the elements to obtain structures with multiple stable configurations. By increasing the number of bistable elements, structures with a large number of different configurations can be designed. A particular attraction of this approach is that it produces structures able to maintain their shape without any power being supplied. The first part of this paper focuses on the design and realization of a low-cost snap-through strut, whose two different lengths provide the required bistable feature. A parametric study of the length-change of the strut in relation to the peak force that needs to be applied by the driving actuators is carried out. Bistable struts based on this concept have been made by injection molding nylon. Next, beamlike structures based on different architectures are considered. It is shown that different structural architectures produce structures with workspaces of different size and resolution, when made from an identical number of bistable struts. One particular architecture, with 30 bistable struts and hence over 1 billion different configurations, has been demonstrated.

Introduction

A requirement that is common to many fields of engineering is the need for low-cost, reliable, reconfigurable structures. Potential applications include robotic manipulator arms, surfaces that control ventilation in buildings, and active facades that control the sunlight entering a building. Additionally, there are applications involving, for example, radioactive or toxic environments where it may be cheaper to use low-cost disposable manipulators than high-cost manipulators that have to be decontaminated after use.

Focusing on robotic manipulators, the relatively high cost of traditional devices results from the use of continuous actuation and the ancillary need for feedback control systems. A novel approach to these requirements is to combine two known structural concepts: a variable geometry truss and a bistable structural element.

Variable geometry trusses (VGTs) were first introduced in the context of cranelike devices that could be used to help build large orbital stations or planetary exploration vehicles [1,2]. A VGT is a three-dimensional assembly of struts connected only at the ends (hence a *truss* structure), whose configuration is determined by the length of the struts. For the configuration of the structure to be *uniquely* determined by the lengths of the struts, kinematically determinate architectures are adopted. Similarly, statically determinate architectures are adopted to ensure that any change in length of the struts does not induce stresses in the structure, i.e., the structure does not fight against the imposed change in length of the strut [3].

The idea of using bistable structural elements in robotic devices was proposed quite some time ago [4,5]. Further work has been done in the area in the last ten years, especially at MIT [6–8] and Johns Hopkins University [9–11]. As has been recognized by previous researchers, if the number of bistable elements in a VGT is large enough, the freedom of movement of the truss approaches that of a system with continuous actuators. However, the control requirements for the binary VGT would be much simpler, as the current configuration of the structure would be determined simply by the state of its bistable elements.

The majority of the work done at Johns Hopkins University has been focused on the macroscopic control of VGTs, such as forward and inverse kinematics. Prototype trusses have been built using pneumatic actuators as bistable elements. The research presented in this paper was motivated by the need to provide bistable structural elements that may be coupled with the Electrostrictive Polymer Artificial Muscles (EPAM) actuators that have been developed in the Field and Space Robotics Laboratory at MIT. Compared with pneumatic actuators, EPAMs have the potential of being cheaper and lighter, as well as avoiding the requirement for compressed air lines.

This paper consists of two parts. The first part focuses on the design and realization of a low-cost snap-through strut, whose two different lengths provide the required bistable feature. A parametric study of the change in length (i.e., the stroke) of the strut in relation to the peak force that needs to be applied by the driving actuators is carried out. Bistable struts based on this concept have been made by injection molding nylon.

In the second part, beamlike structures based on different VGT architectures are considered. It is shown that different structural architectures produce structures with workspaces of different size and resolution when the same number of identical bistable struts are incorporated into these structures. The only actuation that is required is that needed to flip the struts between their two states. One particular architecture, with 30 bistable struts and hence around 10^9 different configurations, has been demonstrated by means of a physical model.

Von Mises Truss

The proposed bistable snap-through strut is based on the simple two-bar structure shown in Fig. 1a. The apex joint has an initial rise w_0 and the two bars have equal initial lengths. This is a well-known structure, known as the von Mises truss.

Assuming that the struts are initially straight, that their Euler buckling load is so large that they never buckle, and furthermore that they remain linear-elastic throughout, the deformation is symmetric. The classical analysis of the von Mises truss (see [12,13] for details) gives the following relationship between the applied load, $2F$, and the rise of the apex from a horizontal line through the side joints, w, defined as positive downwards:

$$F = -EA\left(\frac{1}{\sqrt{w^2 + L^2}} - \frac{1}{\sqrt{w_0^2 + L^2}}\right)w \tag{1}$$

where EA is the axial stiffness of the inclined elements.

Presented as Paper 1529 at the 45th SDM Conference, Palm Springs, CA, 19–22 April 2004; received 25 March 2005; revision received 18 July 2006; accepted for publication 17 September 2006.

*Research Student, Department of Engineering, Trumpington Street. Current Address: CERN, European Organization for Nuclear Research, CH-1221 Geneva 23, Switzerland.

†Professor of Structural Engineering, Department of Engineering, Trumpington Street; pellegrino@eng.cam.ac.uk. Associate Fellow AIAA.

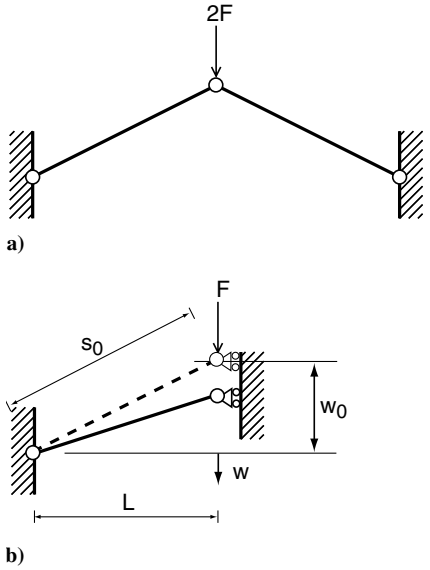

Fig. 1 Von Mises truss.

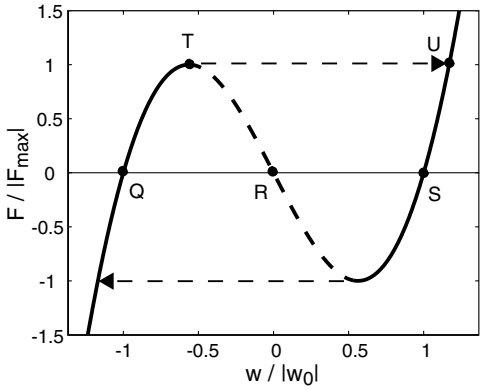

Fig. 2 Force vs rise of a typical Mises truss.

Plotting the equilibrium path, i.e., the locus (w, F) of equilibrium configurations/loads, produces the characteristic up-down-up path shown in Fig. 2. Note that both axes have been normalized, the x-axis with respect to w_0 and the y-axis with respect to $F_{\max}$; this is the magnitude of F at which the slope of the path becomes zero. Also note that the unstable part of the path, where $\mathrm{d}F/\mathrm{d}w < 0$, has been shown dashed.

In the figure, points Q and S, with $w = \pm w_0$, correspond to two different, stable configurations of the structure when $F = 0$. There is also a third equilibrium configuration, point R, which, however, is unstable. Hence, it can be concluded that the von Mises truss is a bistable structure.

Next, we will consider the process through which the structure jumps from one configuration to the other. Consider the behavior of the structure starting from the initial configuration shown in Fig. 1a, which corresponds to point Q in Fig. 2. As the downwards, positive F is gradually increased, the struts are initially under compression. When F reaches the maximum value, $F_{\max}$, the truss jumps from point T to point U, where it can support increasing values of F through tension in the struts.

Snap-Through Strut

Geometry

A bistable structure with the same snap-through behavior of the von Mises truss is shown in Fig. 3. The idea is to use a pair of identical von Mises trusses, which provide the required snapping behavior, to connect the two stiff elements AG and CFHE. The reason why a pair of trusses is used, instead of only one, is to constrain element AG against rotation. Out-of-plane stiffness is imparted by giving the

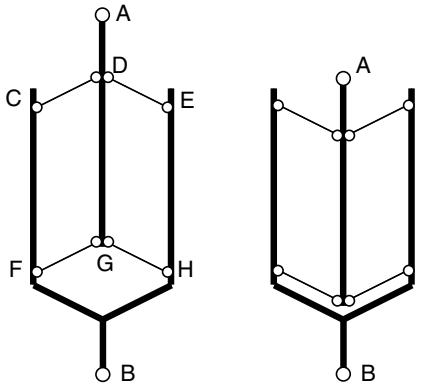

Fig. 3 Concept of snap-through strut.

structure some depth; this means that the pin-jointed connections shown in the diagram are in fact revolute joints. Hence, in three dimensions each joint allows only a single degree of rotational freedom about an axis orthogonal to the plane of the diagram. However, although attractive, this concept has some important limitations.

A key problem is that snap-through struts designed in such a way as to satisfy all of the assumptions of the classical von Mises truss analysis, e.g., the elements CD, DE, etc., do not buckle or yield, have relatively small axial stiffness in comparison with the force at which they snap through. This follows from the smooth variation of F with w, as shown in Fig. 2, which leads to a gradual reduction in the stiffness of the structure even for small changes of w. Another problem is that only relatively small values of w_0 can be accommodated without inducing large strains in the material. This is an important limitation, because $2w_0$ is the *stroke* of the strut.

An alternative is to design struts with much larger values of $2w_0$, but made from thin elements that buckle elastically (similar concepts have been proposed for MEMS devices [14,15]). Such struts will snap by *bifurcation buckling* instead of by reaching a *limit point*, and their design involves considering the Euler buckling load of the inclined elements. This approach affords much greater freedom to the designer, and allows the snap-through load of a relatively stiff von Mises truss to be reduced to the required level. A typical plot of F vs w for a truss whose members are allowed to buckle as classical Euler struts is shown in Fig. 4.

Another alternative is to insert stops that limit the travel of the moving element AG. This has the advantage of conferring higher stiffness at the cost of some complexity in the design, and a reduction in the stroke of the snap-through strut.

Maximum Force

In most practical designs of snap-through struts, the inclined elements CD, DE, etc., buckle very early on. This observation can be exploited to set up a simple analytical model that predicts the maximum force that can be supported by a snap-through strut.

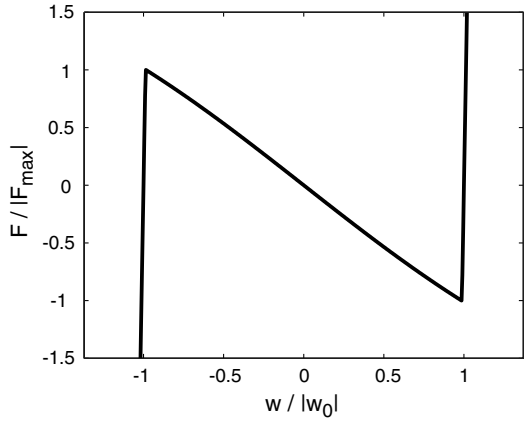

Fig. 4 Force vs rise of von Mises truss with elements allowed to buckle.

The maximum axial force in the members CD, DE, FG, GH is their Euler buckling load, P_E, where

$$P_E = \frac{\pi^2 EI}{s_0^2} \tag{2}$$

The maximum force on the strut, $4F_{\max}$, is readily obtained from vertical equilibrium, which gives

$$F_{\max} = P_E \frac{w}{s} \tag{3}$$

and, assuming the inclined elements to have rectangular cross section of height t and breadth b

$$F_{\max} = \frac{\pi^2 Ebt^3}{12 s_0^2} \frac{w}{s} \tag{4}$$

An approximate expression for $F_{\max}$ can be obtained with the assumption that the vertical movement of the apex joint before buckling is negligible, so that $s \approx s_0$ and $w \approx w_0$, then

$$F_{\max} \approx \frac{\pi^2 Ebt^3}{12} \frac{w_0}{(w_0^2 + L^2)^{\frac{3}{2}}} \tag{5}$$

To find the value of w_0 that produces the maximum possible value of $F_{\max}$, for any given material and cross-sectional dimensions, consider

$$\frac{\mathrm{d}F_{\max}}{\mathrm{d}w_0} = \frac{\pi^2 Ebt^3}{12} \frac{(w_0^2 + L^2)^{\frac{3}{2}} - 3w_0^2(w_0^2 + L^2)^{\frac{1}{2}}}{(w_0^2 + L^2)^3} \tag{6}$$

Setting $\mathrm{d}F_{\max}/\mathrm{d}w_0 = 0$ gives

$$(w_0^2 + L^2)^{\frac{3}{2}} = 3w_0^2(w_0^2 + L^2)^{\frac{1}{2}} \tag{7}$$

from which

$$w_0 = L/\sqrt{2} \tag{8}$$

Substituting Eq. (8) into Eq. (5) gives the corresponding value of $F_{\max}$, hence

$$\max(F_{\max}) = \frac{\pi^2}{18\sqrt{3}} \frac{Ebt^3}{L^2} \tag{9}$$

For design purposes it is useful to consider the ratio $F_{\max}/\max(F_{\max})$, which has been plotted against w_0/L in Fig. 5.

The preceding analysis can be refined by accounting for the shortening of the inclined elements, but this time the solution is not in closed form. The results of the numerical solution, for several values of t/L, have been plotted in Fig. 6. This figure shows that for high values of w_0/L, inclined elements with t/L up to 0.1 still approximate closely to inextensional elements for the purpose of estimating $F_{\max}$. At lower values of w_0/L the approximation is less good and an analysis considering the extension of these elements is required to get an accurate estimate for $F_{\max}$.

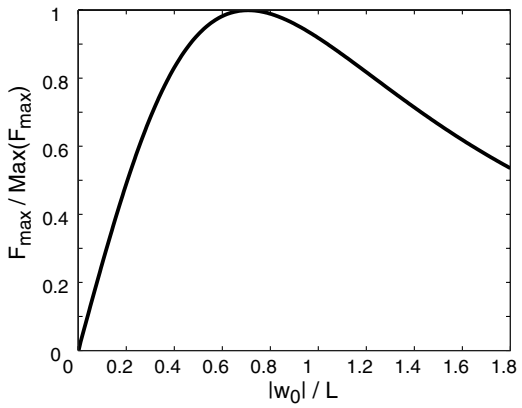

Fig. 5 Variation of snapping force, assuming inextensional behavior.

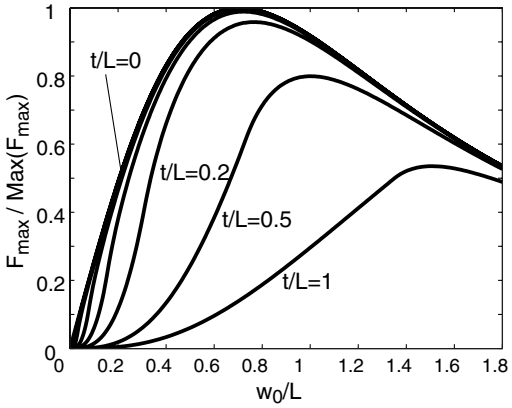

Fig. 6 Variation of snapping force, accounting for extension.

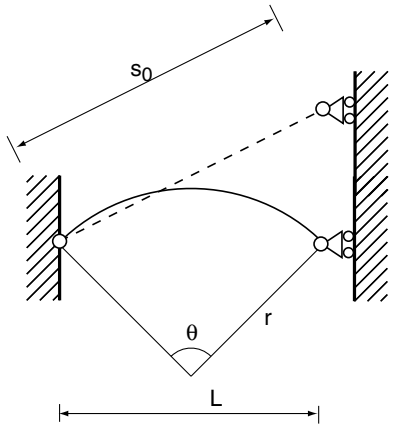

Fig. 7 Configuration of maximum strain.

Constraint Due to Yielding

It is also necessary to ensure that the maximum strains induced in the structural members remain lower than the yield strain of the material. For any design of the strut, the maximum strain occurs when the ends of the inclined elements are closest to each other, and hence when $w = 0$ as shown in Fig. 7. Assuming the inclined elements to be slender, the strains along the centerline can be neglected in comparison with the maximum bending strains. Also, it is assumed that the apex joint moves only vertically and that the elements deform into circular arcs.

The bending strains can be calculated from

$$\varepsilon = \frac{t}{2r} \tag{10}$$

where

$$L = 2r \sin\frac{\theta}{2} = 2r \sin\frac{s_0}{2r} \tag{11}$$

Rearranging Eq. (11) gives

$$r = \frac{L/2}{\sin(s_0/2r)} \tag{12}$$

which can be solved iteratively to find r for any given value of L and w_0. Once r is known, ε can be found using Eq. (10). Figure 8 shows a plot of ε against w_0. The design for which the maximum strain is largest is that for which the inclined elements form semicircles when $w = 0$. Hence, the values of the parameters defined in Fig. 7 are $\theta = \pi$, $L = 2r$, and $s_0 = \pi r$, and so

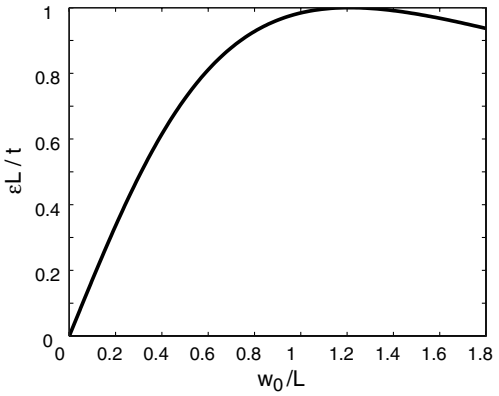

Fig. 8 Maximum bending strain during snap through.

$$w_0 = \sqrt{s_0^2 - L^2} = r\sqrt{\pi^2 - 4} \approx 1.211L \tag{13}$$

Asymmetric Buckling

So far it has been assumed that the von Mises trusses that make up the snap-through strut buckle symmetrically. Although the snap through of the classical von Mises truss is indeed symmetric, it is not obvious that this is still the case when the members are allowed to buckle.

We are interested in the question of symmetry for two reasons. Firstly, we want to know whether or not $F_{\max}$ might be reduced. Secondly, if the behavior is asymmetric, this would have to be taken into account when calculating the maximum strain.

Regarding the first question, because the structure remains symmetric until at least one member reaches the Euler buckling load, it can be concluded that Eq. (5) is correct, provided that the inclined elements are initially straight.

The question of whether the structure remains symmetric in the postbuckling regime requires a more detailed analysis. Figure 9a shows a von Mises truss in a symmetric state where w is fixed. Depending on the value of w, the inclined elements may be either in tension or compression, and may of course be buckled.

To examine the stability of the symmetric configuration, we will consider a small horizontal displacement, δu. For stability, the horizontal stiffness has to be positive, and hence

$$\frac{\mathrm{d}F_H}{\mathrm{d}u} > 0 \tag{14}$$

In general, F_H is the resultant of F_{HL} and F_{HR}, i.e., the horizontal components of the forces acting on the left- and right-inclined elements, respectively. Figure 9b shows the right-hand inclined element of the truss, as the apex joint is moved a distance δu to the right. From horizontal equilibrium

$$F_{HR} = P_R \cos\phi_R \tag{15}$$

where P_R denotes the force acting on the right-hand element. Differentiating Eq. (15),

$$\frac{\mathrm{d}F_{HR}}{\mathrm{d}u} = \frac{\mathrm{d}P_R}{\mathrm{d}u}\cos\phi_R + P_R\frac{\mathrm{d}(\cos\phi_R)}{\mathrm{d}u} \tag{16}$$

Notice, from Fig. 9b, that

$$\frac{\mathrm{d}s_R}{\mathrm{d}u} = \cos\phi_R \tag{17}$$

hence we can rewrite the first term on the right-hand side of Eq. (16) as

$$\frac{\mathrm{d}P_R}{\mathrm{d}u}\cos\phi_R = \frac{\mathrm{d}P_R}{\mathrm{d}s_R}\frac{\mathrm{d}s_R}{\mathrm{d}u}\cos\phi_R = \frac{\mathrm{d}P_R}{\mathrm{d}s_R}\cos^2\phi_R \tag{18}$$

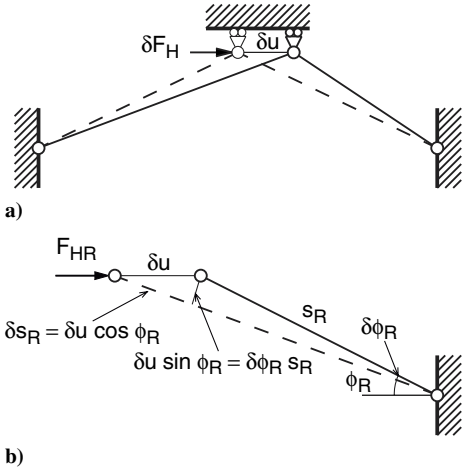

Fig. 9 a) Horizontal perturbation of von Mises truss and b) right-hand inclined element.

Regarding the second term, note from Fig. 9b that

$$\frac{\mathrm{d}\phi_R}{\mathrm{d}u} = \frac{\sin\phi_R}{s_R} \tag{19}$$

hence

$$\frac{\mathrm{d}\cos\phi_R}{\mathrm{d}u} = \frac{\mathrm{d}\cos\phi_R}{\mathrm{d}\phi_R}\frac{\mathrm{d}\phi_R}{\mathrm{d}u} = -\frac{\sin^2\phi_R}{s_R} \tag{20}$$

Substituting Eqs. (18) and (20) into Eq. (16), we get

$$\frac{\mathrm{d}F_{HR}}{\mathrm{d}u} = \cos^2\phi_R\frac{\mathrm{d}P_R}{\mathrm{d}s_R} - P_R\frac{\sin^2\phi_R}{s_R} \tag{21}$$

The same approach can of course be applied to the left-hand inclined element to obtain an equivalent expression for F_{HL}. Then, because F_H is the sum of F_{HL} and F_{HR}

$$\frac{\mathrm{d}F_H}{\mathrm{d}u} = \frac{\mathrm{d}F_{HL}}{\mathrm{d}u} + \frac{\mathrm{d}F_{HR}}{\mathrm{d}u} = \cos^2\phi_R\frac{\mathrm{d}P_R}{\mathrm{d}s_R} + \cos^2\phi_L\frac{\mathrm{d}P_L}{\mathrm{d}s_L} - P_R\frac{\sin^2\phi_R}{s_R} - P_L\frac{\sin^2\phi_L}{s_L} \tag{22}$$

Exploiting the fact that the structure remains geometrically essentially unchanged and symmetric until it buckles, $\phi_L = \phi_R \approx \phi_0$, $s_L = s_R \approx s_0$, and $P_L = P_R$ (the common value will be denoted by P). Hence Eq. (22) can be simplified to

$$\frac{\mathrm{d}F_H}{\mathrm{d}u} = \cos^2\phi_0\left(\frac{\mathrm{d}P_R}{\mathrm{d}s_R} + \frac{\mathrm{d}P_L}{\mathrm{d}s_L}\right) - 2P\frac{\sin^2\phi_0}{s_0} \tag{23}$$

The simplest way of showing that the postbuckling behavior of the snap-through strut is symmetric throughout is to first determine the symmetric configuration where $\mathrm{d}F_H/\mathrm{d}u$ is smallest, and then check the sign of $\mathrm{d}F_H/\mathrm{d}u$ in this particular configuration. Because the snap-through strut contains two von Mises trusses, the lateral stability of each truss has to be analyzed separately. Minimizing Eq. (23) requires maximizing P and ϕ_0 while minimizing $\mathrm{d}P_R/\mathrm{d}s_R$ and $\mathrm{d}P_L/\mathrm{d}s_L$.

Let us start with a truss with perfect, slender inclined elements in an unloaded state. P is equal to zero, and the axial stiffness of the inclined elements is

$$\frac{\mathrm{d}P_R}{\mathrm{d}s_R} = \frac{\mathrm{d}P_L}{\mathrm{d}s_L} \approx \frac{AE}{s_0} \tag{24}$$

As we increase the vertical load on the truss, initially the axial stiffness of the inclined elements does not change, but when P_R and/or P_L reach the critical Euler buckling load, then the axial stiffness of the element that buckles suddenly changes to

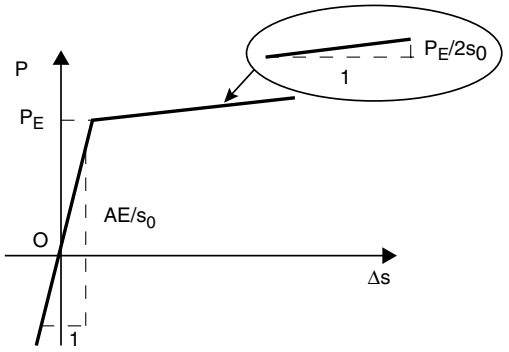

Fig. 10 Pre- and postbuckled axial stiffness.

$$\frac{dP_L}{ds_L} = \frac{P_E}{2s_0} \quad \text{and/or} \quad \frac{dP_R}{ds_R} = \frac{P_E}{2s_0} \tag{25}$$

The preceding result, summarized in Fig. 10, is based on a standard small-rotation, asymptotic expansion of the postbuckling behavior of a beam-column [13,16]. Note that this postbuckled stiffness is much smaller than the prebuckled value. As an example, inclined elements with the properties given in Table 1 have a prebuckling stiffness, from Eq. (24), that is 1097 times higher than the postbuckling stiffness, from Eq. (2) and (25). Hence, clearly the horizontal stiffness of a von Mises truss is much reduced once buckling occurs.

As $|w|$ is further decreased, the horizontal stability generally increases, as the dominant terms in Eq. (22) are the $\sin^2$ terms, which decrease more rapidly than P increases. Thus, the critical configuration is the one that occurs immediately after the onset of buckling, and the smallest horizontal stiffness is obtained when both inclined elements are buckled. Hence, substituting Eq. (25) into Eq. (23) gives

$$\frac{dF_H}{du} = \frac{P_E}{s_0}(\cos^2\phi_0 - 2\sin^2\phi_0) \tag{26}$$

It follows that $dF_H/du > 0$, and hence the truss is horizontally stable when symmetric, for

$$\phi_0 < \tan^{-1}\sqrt{\frac{1}{2}} = 35.3 \text{ deg} \tag{27}$$

If, instead of being perfectly straight, the inclined element has an initial bow, the axial loads in the inclined elements will be reduced and the minimum value of dP_R/ds_R will be increased. Both of these effects will increase the stability of the symmetric configurations, and hence it can be concluded that for trusses made from linear-elastic material, Eq. (27) provides a bound, below which all trusses will behave in a symmetric manner.

Physical Realization

To provide an effective demonstration of the proposed concept, a key requirement was to design a snap-through strut with a large stroke relative to its overall length. This called for a material with high yield strain, both for the inclined elements and the "living" hinges.

Table 1 Snap-through strut prototype characteristics

Symbol	Description	Value
b	Width of plate	5 mm
E	Young's modulus	3000 N/mm^2
L	Half span of truss	7 mm
t	Plate thickness	0.35 mm
w_0	Rise of truss	2 mm
	Length of hinge section	0.4 mm
	Thickness of hinge section	0.15 mm

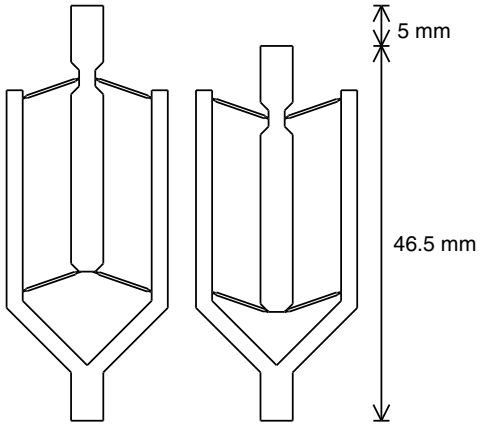

Fig. 11 Design of snap-through strut prototype.

A suitable material is Nylon 6, and it was decided to injection-mold the whole strut as a single piece (apart from the transverse straps, described in the following paragraph). Figure 11 shows a sketch of the chosen design. The characteristics of this strut are set out in Table 1. Note that in this particular implementation the strut has a stroke of about 5 mm, corresponding to about 10% of its overall length.

Figure 12 shows a complete prototype, including the injection-molded internal piece and four straps, two on each face of the strut, glued to the side members. The straps prevent lateral movement of the side walls when the inclined elements are placed under compression; without the straps, the side members would simply bend outwards and the snap-through behavior would be lost.

Several snap-through struts were tested in a materials testing machine. Figure 13 shows a typical, measured force-displacement relationship; here the upper dotted line corresponds to the strut being shortened and the lower dotted line to the strut being extended. The theoretical response, derived by assuming linear-elastic axial shortening and Euler buckling of the inclined elements, is shown by a solid line.

As can be seen, the analytical model gives quite good results, but does not capture the difference between the extension and shortening curves. To explain and model this behavior a more realistic, viscoelastic model of nylon is required; a more detailed analysis can be found in [17]. It is, however, confirmed that the strut does have two stable configurations and if moved from one will either return to it or jump to the alternative configuration.

Fig. 12 Prototype.

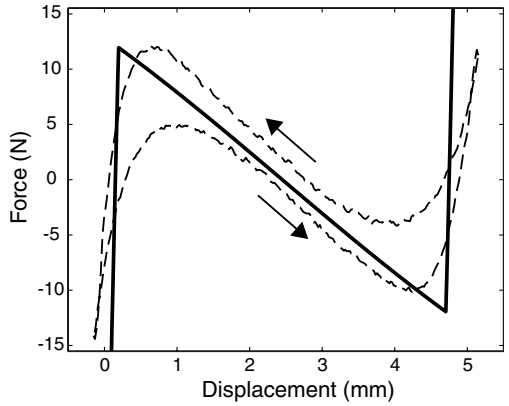

Fig. 13 Theoretical and experimental behavior of nylon strut.

Multiconfiguration Structures

Evaluation of Workspace

A space frame architecture suitable for a VGT must be both statically and kinematically determinate [3]. If this is not the case, the structure will either be a mechanism, and hence too floppy for most practical applications, or it will develop a state of self-stress opposing actuation, when the length of its members is changed.

Only trusses with repeating units were considered, to simplify the process of constructing low-cost physical demonstrators. Figure 14 shows three architectures that were considered; in each case a unit cell is highlighted. Three elements of each unit cell were replaced with snap-through struts.

Figure 14a shows a structure made up of a number of octahedra. This is a common geometric unit in space structures and has been researched extensively [1,2]. It has the advantage that all of its members have equal length; another advantage is that of having end faces normal to the axis of the structure. The snap-through struts were placed in three of the six elements that connect the triangles that lie in horizontal planes (as in a Stewart platform).

Figure 14b shows a structure made up of tetrahedra. The highlighted unit cell is made up of three such tetrahedra. The snap-through struts were located along the three helices that form the edges of this structure.

Figure 14c is another tetrahedral truss which has been "untwisted" by extending some of the elements. As this truss form is frequently used in the booms of tower cranes, this truss type will be referred to as a crane structure. In each unit cell there is now one element that is $\sqrt{2}$ times longer than all of the other elements. Additionally, every other diagonal bracing element has been rotated by 90 deg. Hence, two unit cells rather than one have been highlighted. Here, the snap-through struts have been located in all of the vertical elements in the truss.

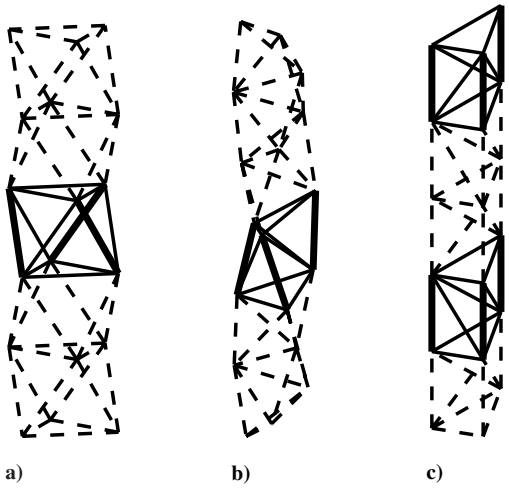

Fig. 14 Three space frame architectures, with unit cells shown by solid lines. Thicker lines indicate the location of the snap-through struts.

Space frames made up of ten units, based on each of these three architectures, were compared with the aim of finding the structure that has the largest possible workspace as well as the most regular distribution of points within the workspace. Having a large workspace is beneficial as it allows the truss to manipulate objects over a larger area. Having uniformly spaced points is advantageous as it means that inside the workspace a good approximation to any given point is likely to be found.

Because of the relatively short overall length of these structures, their workspaces extend mainly in two dimensions and are rather thin in the third dimension. If the length of the structures is increased by adding more and more units, they will be able to bend back on themselves and thus reach a "volume" of points. If a short truss has the ability to reach a relatively large area it means that it has the ability to exhibit a relatively large curvature, and the same functionality is also required for a larger truss to achieve a large work volume.

Each of the three structures incorporates 30 snap-through struts and thus each has $2^{30} \approx 1.07 \times 10^9$ unique configurations. Around 10,000 of these were plotted for each structure and superimposed on top of each other (see Fig. 15). Note that for each structure, the snap-through struts were defined as having a length of either 1 or 1.1. As can be seen from Fig. 15, the crane structure gives the best spread of points; it was therefore decided to use this design for the manufacture of a working prototype.

Prototype Structure

A ten-unit crane structure was constructed using snap-through struts and lightweight polymer tubing and joints from the

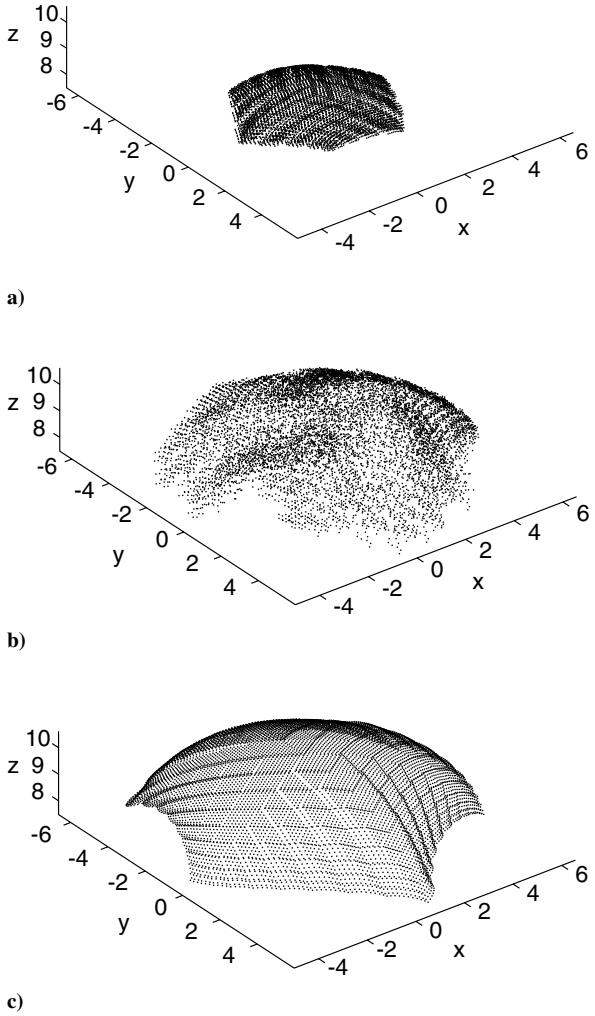

Fig. 15 Workspaces of three different trusses: a) octahedral, b) tetrahedral, c) crane.

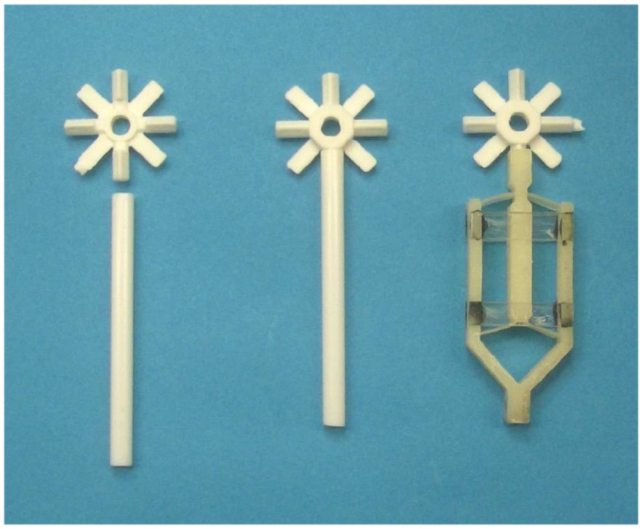

Fig. 16 Modeling kit used to build the prototype.

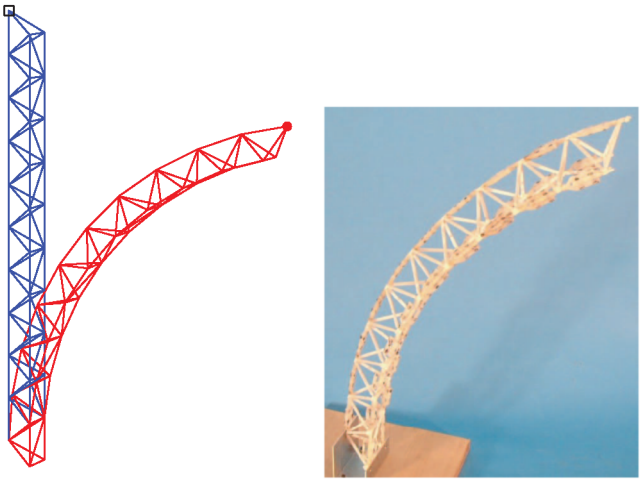

a) **b)**

Fig. 17 Actuated state of truss: a) kinematic model; b) prototype.

Microframe Kit by Tecna Display. Details are shown in Fig. 16. The prototype structure has a total mass of 87 g and a length of 557 mm.

Figure 17 shows a photo of the prototype where all of the elements along one side have been actuated. For the purposes of comparison, a kinematic simulation that predicts any configuration of the structure is also shown; details can be found in [17]. It can be seen that the two shapes correlate well. Note that all snap-through struts are nominally identical to those described in the section "Physical Realization"; also note that in the prototype each strut is actuated by hand.

For a more detailed comparison, the predicted total horizontal displacement of the prototype was 319 mm as opposed to the measured value of 338 mm. Imperfections in manufacturing the model, as well as ignoring gravity effects account for this small discrepancy. What is more significant, though, is that the prototype displays the expected shape.

Conclusions

A novel, bistable structural element based on the snap-through properties of the von Mises truss has been presented in this paper. This element, the snap-through strut, consists of a stiff, U-shaped piece connected to a stiff plunger by four thin, inclined plates. When a sufficiently large compression force is applied to the snap-through strut, the plates suddenly buckle, allowing the plunger to move further into the U-shaped piece, and thus reach an alternative configuration. The strut maintains the shorter configuration until a sufficiently large tensile force is applied.

A simple analysis of the maximum compressive force that can be applied to the snap-through strut without causing it to snap to the alternative stable configuration has been presented, initially assuming the behavior of this element to be symmetric. On this basis, an estimate of the maximum strain that the plates have to withstand without permanent deformation has been obtained. Based on this analysis, we have derived general expressions of these quantities, in terms of four design parameters: the rise, thickness, breadth, and length of the plates. These expressions can be used for design purposes.

An alternative approach would be to use bistable struts with inclined plates that are initially bowed, as, for example, in [18], to decrease the force required to snap the strut.

An analysis of the stability of the assumed symmetric buckling and postbuckling behavior of the snap-through strut has shown that, for linear-elastic material response, the assumed symmetric buckling mode is in fact symmetric for a rise angle less than 35.3 deg. This result is not valid for nonlinear material behavior, as in this case $\mathrm{d}P_R/\mathrm{d}s_R$ and $\mathrm{d}P_L/\mathrm{d}s_L$ can no longer be calculated using Eq. (25) and a more general analysis is needed [17]. Indeed, asymmetric response was observed during tests carried out on snap-through struts made of nylon, with a rise angle of about 16 deg. The asymmetry leads to higher maximum strains in the inclined plates, but does not affect the maximum compressive load before snap through.

These snap-through struts have been incorporated into space frames with several different configurations, and, although by no means exhaustive, our search (restricted to structures that are both statically and kinematically determinate) has shown a "crane" truss to be the best. A prototype arm was constructed to this design and was found to display the shape characteristics predicted using a kinematic simulation.

Finally, it should be noted that the study of asymmetric buckling modes presented in this paper did not consider the possibility of the bottom Mises truss moving differently from the upper truss. This alternative buckling mode has been investigated in [17] and has been found to be of no practical consequence.

Acknowledgments

Financial support from the Cambridge-MIT Institute (CMI) is gratefully acknowledged. T. S. thanks the Engineering and Physical Sciences Research Council for the award of a studentship and the Cambridge Newton Trust for additional support. We thank Stephen Dubowsky for inspiring our work on bistable structures, and for advice on the present research. An earlier version of this paper was presented at the 38th AIAA SDM Conference.

References

[1] Miura, K., "Variable Geometry Truss Concept," The Institute of Space and Astronautical Science, Sagamihara, Japan, Report No. 614, 1984.

[2] Rhodes, M., and Mikulas, M. M., Jr., "Deployable Controllable Geometry Truss Beam," NASA Technical Memorandum 86366, 1985.

[3] Pellegrino, S., and Calladine, C. R., "Matrix Analysis of Statically and Kinematically Indeterminate Frameworks," *International Journal of Solids and Structures*, Vol. 22, No. 4, 1986, pp. 409–428.

[4] Anderson, V. C., and Horn, R. C., "Tensor Arm Manipulator Design," ASME Paper 67-DE-57, 1967.

[5] Roth, B., Rastegar. J., and Scheinman, V., "On the Design of Computer Controlled Manipulators," *First CISM-IFTMM Symposium on Theory and Practice of Robots and Manipulation*, 1973, pp. 93–113.

[6] Lichter, M., "Concept Development for Lightweight Binary-Actuated Robotic Devices, with Application to Space Systems," M.S. Thesis, Massachusetts Institute of Technology, Cambridge, MA, Chap. 2, 2001.

[7] Wingert, A., Lichter, M., Dubowsky, S., and Hafez, M., "Hyper-Redundant Robot Manipulators Actuated by Optimized Binary Dielectric Polymers," *Proceedings of SPIE: The International Society for Optical Engineering*, Vol. 4695, 2002.

[8] Sujan, V. A., Lichter, M., and Dubowsky, S., "Lightweight Hyper-Redundant Binary Elements for Planetary Exploration Robots," *Proceedings of the 2001 IEEE/ASME International Conference on Advanced Intelligent Mechatronics*, 2001.

[9] Chirikjian, G., "A Binary Paradigm for Robotic Manipulators,"

Proceedings of the IEEE International Conference on Robotics and Automation, Vol. 4, 1994, pp. 3063–3069.
[10] Ebert-Uphoff, I., and Chirikjian, G. S., "Inverse Kinematics of Discretely Actuated Hyper-Redundant Manipulators Using Workspace Densities," *Proceedings of the IEEE International Conference on Robotics and Automation*, 1996, pp. 139–145.
[11] Lees, D., and Chirikjian, G. S., "An Efficient Method for Computing the Forward Kinematics of Binary Manipulators," *Proceedings of the IEEE International Conference on Robotics and Automation*, 1996, pp. 1012–1017.
[12] Panovko, Y. G., and Gubanova, I. I., "Stability and Oscillation of Elastic Systems: Modern Concepts, Paradoxes and Errors," NASA Technical Translation TT F-751, 1967, Chaps. 2–5.
[13] Bazant, Z. P., and Cedolin, L., *Stability of Structures*, Oxford Univ. Press, Oxford, 1996, pp. 228–231.
[14] Qiu, J., Lang, J., and Slocum, A. H., "A Centrally-Clamped Parallel-Beams MEMS Bistable Mechanism," *Proceedings of the IEEE MEMS-01 Conference*, Interlaken, Switzerland, 2001, pp. 353–357.
[15] Howell, L. L., *Compliant Mechanisms*, Wiley, New York, 2001, pp. 202–205.
[16] Fichter, W. B., and Pinson, M. W., "Load-Shortening Behaviour of an Initially Curved Eccentrically Loaded Column," NASA Technical Memorandum 101643, 1989.
[17] Schioler, T., "Multi-Stable Structural Elements," Ph.D. Dissertation, Univ. of Cambridge, Cambridge, England, 2005.
[18] Plante, J.-S., Santer, M. J., Dubowsky, S., and Pellegrino, S., "Compliant Bistable Di-Electric Elastomer Actuators for Binary Mechatronic Systems," DETC Paper 2005-85576, Sept. 2005.

B. Sankar
Associate Editor